Molecular Dynamics Simulations of an Enzyme Surrounded by Vacuum, Water, or a Hydrophobic Solvent

Martin Norin,* Fredrik Haeffner,‡ Karl Hult,* and Olle Edholm§
*Biochemistry and Biotechnology, ‡Organic Chemistry, and §Theoretical Physics, Royal Institute of Technology, S-100 44 Stockholm, Sweden

ABSTRACT We report on molecular dynamics simulations of a medium-sized protein, a lipase from *Rhizomucor miehei*, in vacuum, in water, and in a nonpolar solvent, methyl hexanoate. Depending on force field and solvent, the molecular dynamics structures obtained as averages over 150 ps had root-mean-square deviations in the range of 1.9 to 3.6 Å from the crystal structure. The largest differences between the structures were in hydrogen bonding and exposed surface areas of the protein. The surface area increased in both solvents and became smaller in vacuum. The change of surface exposure varied greatly between different residues and occurred in accordance with the hydrophobicity of the residue and the nature of the solvent. The fluctuations of the atoms were largest in the external loops and agreed well with crystallographic temperature factors. Root-mean-square fluctuations were significantly smaller in the nonpolar solvents than they were in water, which is in accordance with the notion that proteins become more rigid in nonpolar solvents. In methyl hexanoate a partial opening of the lid covering the active site occurred, letting a methyl hexanoate molecule approach the active site.

INTRODUCTION

This study provides a detailed molecular model of a hydrophobic environment for the *Rhizomucor miehei* lipase and for proteins in general. The properties of biomolecules are affected by the surrounding solvent through van der Waals and electrostatic interactions. Accurate molecular dynamics simulations must include a properly modeled solvent. Molecular force fields have been developed for the simulation of proteins in water solution (Brooks et al., 1983; Hermans et al., 1984; Jorgensen and Tirado-Rives, 1988). Investigations of solvent effects on proteins have been reported (Wong and McCammon, 1986; Levitt and Sharon, 1988; Brooks and Karplus, 1989; Komeiji et al., 1993). In the last decade the use of enzymes as highly specific catalysts in nonaqueous solvents has become widespread in synthesis of organic compounds. The properties of enzymes in such solvents are changed compared to those in water. Examples are increased thermostability (Zaks and Klibanov, 1984), molecular memory for pH (Klibanov, 1986), and altered specificity (Zaks and Klibanov, 1986). For reviews on this subject see, for example, Dordick (1989) and Gupta (1992). However, there are only a few reports of simulations of proteins in nonaqueous media. van Gunsteren and Karplus (1982) made a 25-ps molecular dynamics study of the bovine pancreatic trypsin inhibitor in a nonpolar solvent. De Loof et al. (1992) simulated galanin, a 29-residue hydrophobic neuropeptide in water and 2,2,2-triflouroethanol. Lautz et al.(1990) studied cyclosporin A, a highly hydrophobic cyclic peptide, in both water and a nonpolar solvent. They reported significant deviations between the molecular structures simulated in water and in the nonpolar solvent.

The objective of this study was to increase our understanding of the dynamics of proteins in different environments in general. Of particular interest is the behavior of enzymes in organic solvents. The study also serves as a comparison of molecular dynamics simulations of proteins in vacuum and in solvent. In this paper we report on molecular dynamics simulations of a medium-sized enzyme, *R. miehei* lipase, in vacuum, in water, and in a solution of hydrophobic substrate molecules.

The *R. miehei* lipase is a single-chain (269 residues) protein that belongs to a family of enzymes sharing the α/β hydrolase fold (Ollis et al., 1992). Lipases are enzymes, which hydrolyze triglycerides and liberate fatty acids. The catalytic mechanism of these lipases is similar to that of serine proteases. A catalytic triad, Ser-His-Asp/Glu, is involved in the cleavage of ester bonds. Lipases are activated at hydrophobic surfaces formed by their water-insoluble substrates (Sarda and Desnuelle, 1958). The activation involves movements of one or a few surface loops, which bury the active site in the inactive conformation (Winkler et al., 1990; Brzozowski et al., 1991; van Tilbeurgh et al., 1992; Derewenda et al., 1992a; Grochulski et al., 1993; van Tilbeurgh et al., 1993). The lipase from *R. miehei* has one helix forming a lid over the active site, which opens during activation (Brady et al., 1990; Brzozowski et al., 1991; Derewenda et al., 1992a, b). In addition to hydrolysis of ester groups lipases are also able to catalyze other related nucleophilic substitutions such as alcoholysis and aminolysis in nonaqueous solvents. They are widely used in preparative organic synthesis. The lipase from *R. miehei* shows high activity in various organic solvents (Sonnet and Moore, 1988). In addition the molecular structure of this lipase has been thoroughly investigated by x-ray crystallography (Brady et al., 1990; Derewenda et al., 1992a, b). We have

Received for publication 14 February 1994 and in final form 3 May 1994.
Address reprint requests to Karl Hult, Department of Biochemistry and Biotechnology, Royal Institute of Technology, S-100 44 Stockholm, Sweden. Tel.: 46-8-790-7508; Fax: 46-8-723-1890; E-mail: kalle@biochem.kth.se.

0006-3495/94/08/548/12 $2.00

chosen methyl hexanoate as a model for the hydrophobic solvent given that the lipase is active in this solvent and accepts this compound as a substrate.

MATERIALS AND METHODS

Enzyme reactions

Although the *R. miehei* lipase has been shown to be active in many organic solvents (Sonnet and Moore, 1988; Janssen et al., 1991), we could not find any data in the literature describing reactions catalyzed by the lipase in methyl hexanoate. In order to show that lipase from *R. miehei* is active in methyl hexanoate we performed an enzymatic transesterification between methyl hexanoate and *rac*-1-phenyl ethanol (Fig. 1). Immobilized pure lipase (200 mg) from *R. miehei* (the enzyme preparation was a gift from NOVO Nordisk A/S, Bagsvaerd, Denmark, and it is commercially available as Lipozyme) was mixed with 1 ml (6.8 μmol) of methyl hexanoate and 100 μl (0.83 μmol) of *rac*-1-phenyl ethanol was added. The reaction was performed at 66°C and atmospheric pressure in an open test tube. Samples were taken continuously and were analyzed by gas chromatography. After 3.5 hours about 20% of the added *rac*-1-phenyl ethanol had been converted to the ester product. An initial reaction rate of 1800 μmol/min/g enzyme was observed. No reaction could be detected without the addition of enzyme.

Simulations

All calculations were performed on an Alliant FX2800 computer using the GROMOS program by van Gunsteren and Berendsen (1987), in a version that had been modified to run the most time-consuming subroutines in parallel over several processors. The manual examinations of molecular structures were done using the molecular modeling package SYBYL (Tripos, 1993) running on an Evans & Sutherland ESV33/LCS computer (Salt Lake City, UT). Both the C (charged) and D (uncharged) versions of the GROMOS force field were used in the calculations. In the D version all amino acid residues that may carry net charges were neutral and treated as dipoles. Periodic boundary conditions were applied in all simulations including solvent. Nonbonded interactions were truncated at 10 Å. Bond lengths were constrained using the SHAKE algorithm (Ryckaert et al., 1977). The molecular dynamics simulations were performed at 300 K with a time step of 2 fs. Before performing the molecular dynamics simulations the potential energies of the molecular systems were minimized using 1000 steps of steepest descent minimization. The simulated molecules were first equilibrated for 50 ps followed by a production run of 150 ps during which data were collected for analysis.

Water was described by the simple point charge (SPC) model (Berendsen et al., 1981). Methyl hexanoate was modeled with fractional charges on four atoms as shown in Fig. 2 using standard Lennard-Jones parameters from the GROMOS force field. As for the protein, nonpolar hydrogens were included in the carbons as united hydrocarbon groups. Pure methyl hexanoate (216 molecules) was simulated for 350 ps in a periodic box that was rescaled in size during the first part of the simulation to obtain atmospheric pressure. During the last 200 ps the size of the box was kept fixed, resulting in a density of 0.929 g/cm^3 and a pressure that fluctuated around 1 atmosphere. The interaction energy between the methyl hexanoate molecules was stable at −53.7 kJ/mol. These data may be compared with the experimental density, 0.885 g/cm^3, and the heat of vaporization, 48.04 kJ/mol (Månsson et al., 1977). If the vapor phase of methyl hexanoate is considered as an ideal gas, the heat of vaporization should be equal to the negative value of the interaction energy in the liquid phase plus kT, which gives 56.2 kJ/mol. The

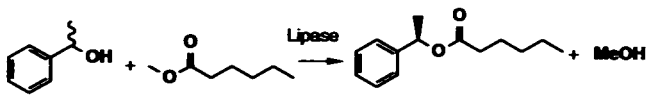

FIGURE 1

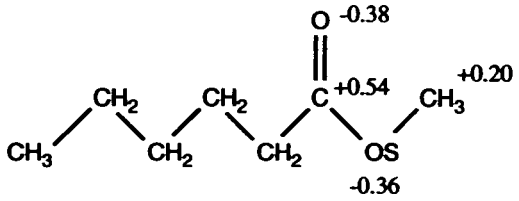

FIGURE 2 Schematic structure of the methyl hexanoate molecules. The GROMOS atoms types are labeled, and point charges used are given.

differences between experimental and calculated values indicate too-strong attractive forces of our model or that the van der Waals radii are too small (or a combination of these parameters). This could be adjusted but we found the accuracy in the present model of methyl hexanoate sufficient for our purposes.

The starting conformation of the enzyme was the crystallographic structure of the closed form of *R. miehei* lipase (Derewenda et al., 1992a). The structure is available in the Brookhaven Protein Data Bank (Bernstein et al., 1977; Abola et al., 1987) with entry number 3TGL. In simulations of the lipase in solvent the protein was centered in a solvent box, and all solvent molecules within a distance of 3 Å from any protein atom were discarded from the system, leaving 5006 or 533 molecules of water and methyl hexanoate, respectively. In both cases about 20% of the total volume was taken up by the protein .

Five simulations were performed using different environments. Two simulations were performed using vacuum conditions, which is a commonly used approximation of the environment of proteins in molecular dynamics simulations. The force fields that were used in the two simulations were the uncharged (D) and charged (C) version of the GROMOS force field, respectively. The simulation of the lipase in water, which modeled the lipase in water solution at neutral pH, used the C version of the force field. It is difficult to obtain a clear picture of the protonation states of the amino acid residues in hydrophobic solvents. Therefore, we performed two simulations of the lipase in methyl hexanoate using either the D or C force field.

The five simulations will be abbreviated in the text as follows: VACU and VACC are the simulations of the lipase in vacuum using the D and C versions of the GROMOS force field, respectively; WTRC is the simulation of the lipase in water using the charged version of the force field; MHEXU and MHEXC are the simulations of the lipase in methyl hexanoate using the D and C versions of the GROMOS force field, respectively.

RESULTS

Structure and dynamics of the solvents

The structure of the methyl hexanoate molecules as monitored by the fraction of gauche bonds did not differ significantly in the presence or absence of the protein. One exception was that five solvent molecules close to the protein had undergone isomerization to the *cis* form in the CH_3-OS-C-CH_2 bond (Fig. 2) in the MHEXC simulation. Given the internal potential of the simulations, the distribution of the *trans*/gauche states of the remaining four bonds did not significantly deviate in any of the simulations from what would be expected for a molecule in dilute gas phase.

The radial distribution functions of methyl hexanoate (MHEXC) and of water (WTRC) around the protein are shown in Fig. 3 *A*. A pronounced first neighbor peak and a weak tendency for a second peak were observed. In the WTRC simulation the first neighbor peak was at different distances from positively, negatively, and uncharged atoms of the protein (Fig. 3 *B*). This effect has been shown by Komeiji et al. (1993), as well as by others.

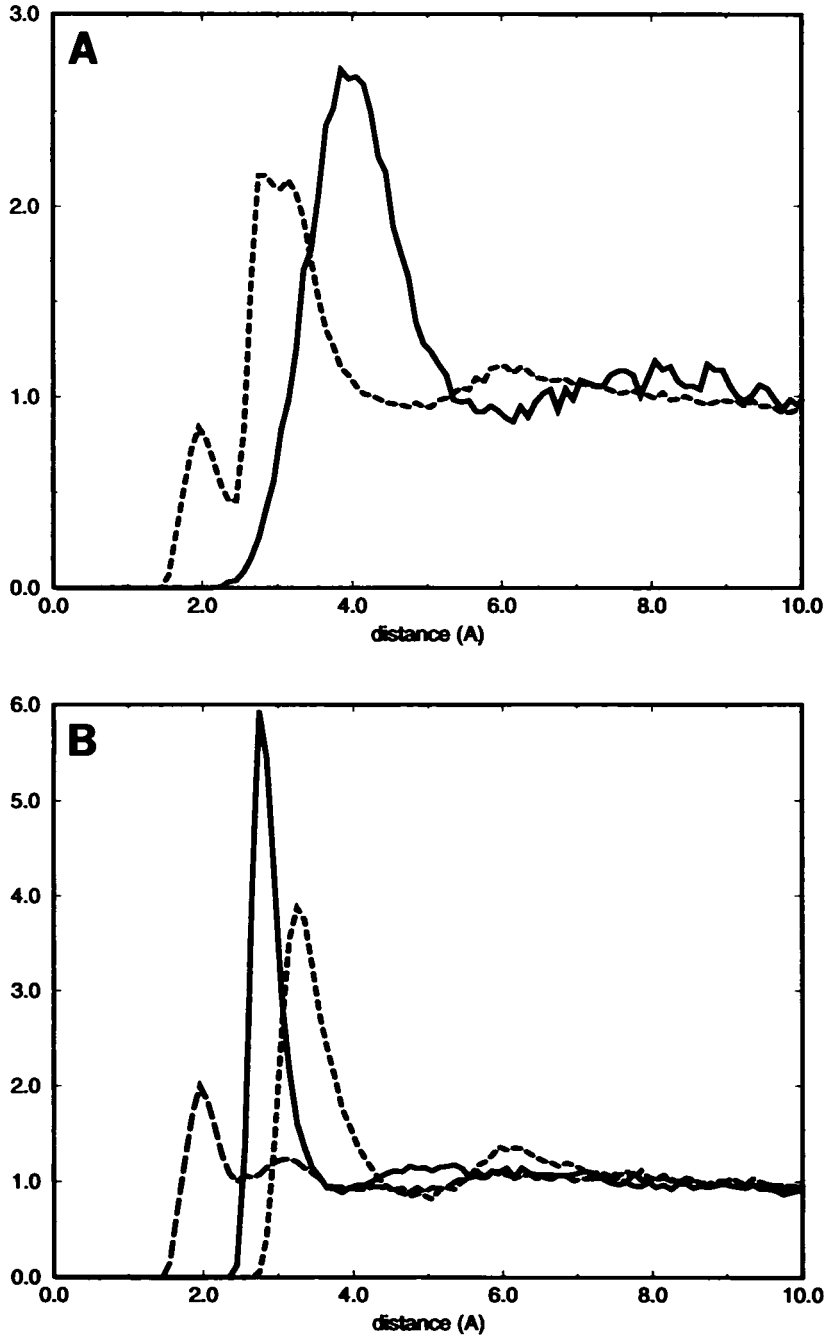

FIGURE 3 Distribution of solvent around the protein. (*A*) Solid line is MHEXC and dashed line is WTRC. (*B*) Distribution of water molecules around positively charged (long dashed line), negatively charged (solid line) and neutral atoms (dashed line).

The orientation of the solvent molecules were calculated as the number of molecules with different angles of the dipole vectors with respect to the vectors from the solvent molecules to the closest protein atom. If the dipole of the solvent molecule is parallel to the vector pointing from the center of mass of the solvent molecule to the closest protein atom, this angle becomes either 0 or 180 degrees, while a perpendicular orientation gives an angle of 90 degrees. We found a tendency for the solvent molecules close to the protein to orient themselves with the dipole vector pointing either toward the protein or away from it as shown in Fig. 4.

The translational diffusion coefficients of the solvent molecules were calculated as a function of the distance from the protein molecule using the relation

$$D = \lim_{t \to \infty} \left[\frac{1}{6t} \langle (\vec{r}(t_0 + t) - \vec{r}(t_0))^2 \rangle_{t_0} \right]$$

$\vec{r}(t_0)$ is the center of mass coordinates at time t_0, and the averaging was done over all solvent molecules and over time t_0.

The translational diffusion coefficient as a function of the distance from the protein is shown in Fig. 5 *A*. The experimental translational diffusion coefficient of water is $2.5 * 10^{-9}$ m^2/s (Hrovat et al., 1980), whereas the model water we use (SPC) has a value equal to $3.6 * 10^{-9}$ m^2/s (Berendsen et al., 1981). Our simulated diffusion coefficient for water distant from the protein agreed with the latter value.

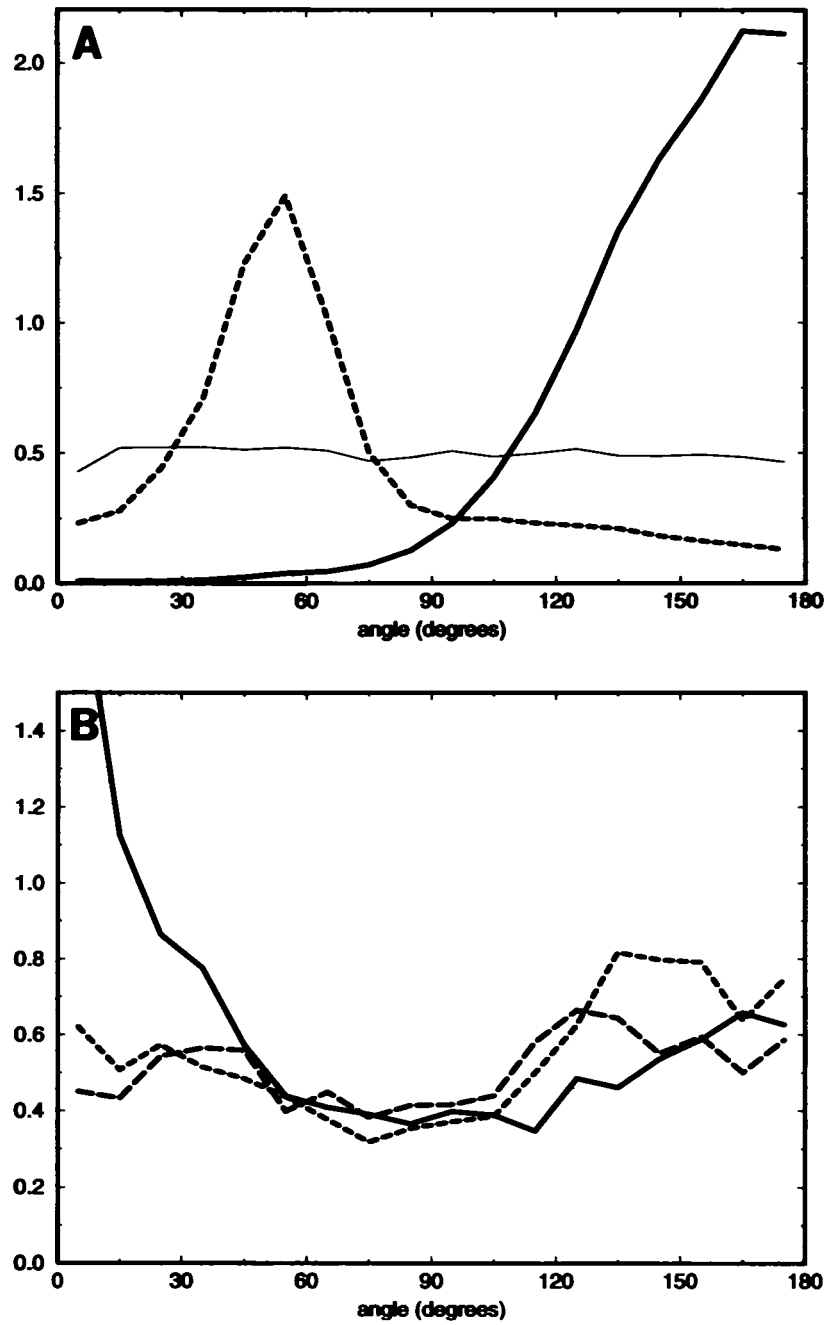

FIGURE 4 Fraction of solvent molecules as a function of the orientation of the solvent dipole. The various curves represent different distances from the protein. (*A*) The WTRC simulation (full line, <3 Å; dashed line, 3–3.5 Å; and thin line, outside 3.5 Å). (*B*) The MHEXC simulation (full, <4 Å; dashed, 4–5 Å; and long dashed outside 5 Å).

In accordance with earlier simulations (Levitt and Sharon, 1988; Brooks and Karplus, 1989; Wong and McCammon, 1986; Komeiji et al., 1993) the translational mobility of the water molecules close to the protein (<5 Å) was slightly reduced. We observed a reduction by a factor of approximately 2 compared with that of distant solvent molecules if a small number of more or less immobilized water molecules (see below) was excluded. Experimentally this has been studied by nuclear magnetic resonance (NMR) spectroscopy (Steinhoff et al., 1993). In the NMR study the reduction of the translational diffusion in the hydration shell around hemoglobin was between three and seven times.

There were eight water molecules more or less bound to the protein during the simulation. They moved only 3 Å during 100 ps, which corresponds to an apparent diffusion coefficient 25 times lower than that of bulk water. All these water molecules were completely buried inside the protein and located at two sites heavily occupied by water molecules in the crystal structure of the protein.

For methyl hexanoate, the calculated translational diffusion coefficient in the bulk was $2.5 * 10^{-9}$ m^2/s. Diffusion close to the protein was four times slower. No significant differences could be observed in the simulations with different charges on the protein as seen from the two lower

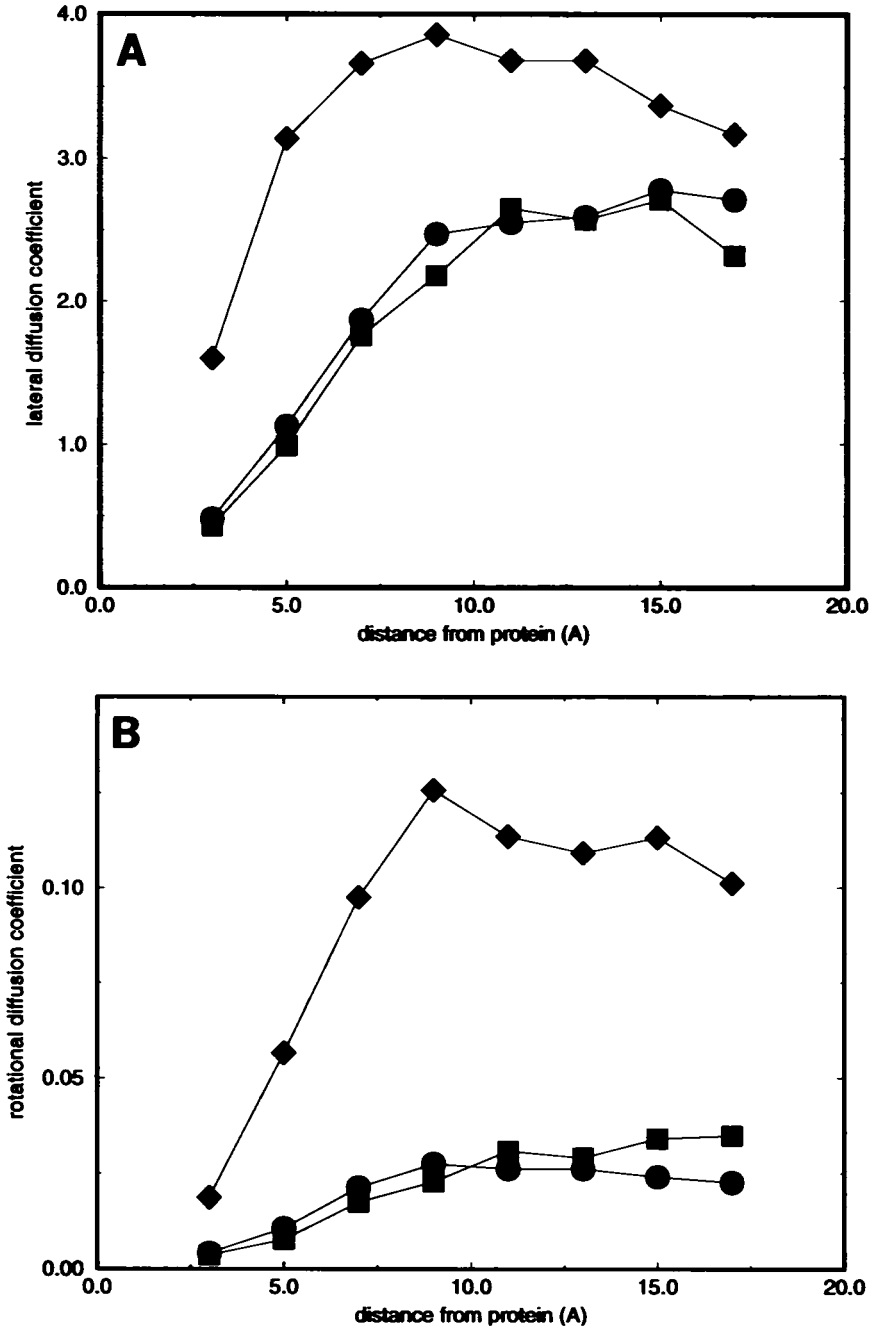

FIGURE 5 Diffusion coefficients of the solvent molecules as a function of the distance from the protein surface. ◆, WTRC simulation; ●, MHEXU simulation; ■, MHEXC simulation. (*A*) Lateral diffusion in $m^2\ s^{-1} * 10^9$. (*B*) Rotational diffusion in $rad^2 ps^{-1}$

curves in Fig. 5.The rotational diffusion is described by the following relation

$$\langle P_\ell[\cos(\theta(t + t_0, t_0))]\rangle = e^{-\ell(\ell+1)Dt}$$

Here, $\theta(t + t_0, t_0)$ is the angle between the orientations at time t and $t + t_0$, and P_ℓ is a Legendre polynomial of the order ℓ. We performed the analysis for $\ell = 1$ or 2 and did not observe any significant difference between the two cases. The rotations of the molecules could not be described by a single exponential function as has been noted by others for bulk water (Wallquist and Teleman, 1991). Two exponent functions gave a perfect fit to the rotational auto correlation function. This may be interpreted as a rotational relaxation originating from two processes. These are one fast jiggling motion within a cage given by neighboring molecules and one slow rotation causing a rearrangement of these molecules.

A rotational diffusion coefficient was calculated from the slower of the two exponentials and is shown in Fig. 5 *B*. The rotational diffusion of water in the 5-Å shell around the protein was five times slower than that of bulk water. The rotation of water is eight times slower in the hydration shell of hemoglobin than in free water as determined by dielectric relaxation (Steinhoff et al., 1993). At long distances from the protein the rotational diffusion coefficient of water was

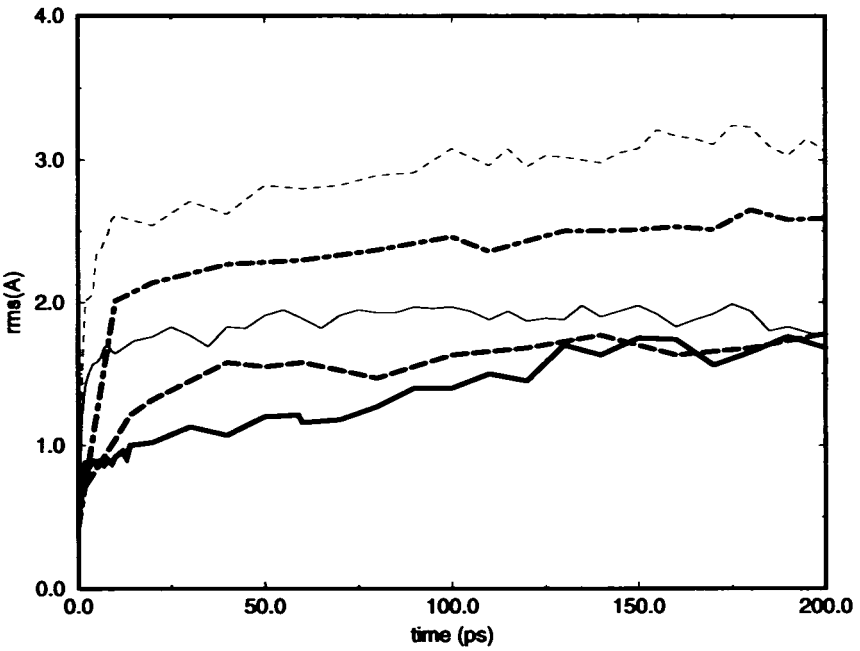

FIGURE 6 The RMS distances from the crystal structure of the Cα atoms in the five simulations as a function of time. Solid thick line is WTRC, solid thin line is VACU, dashed thin line is VACC, dashed thick line is MHEXU, and dashed/dotted line is MHEXC.

$9 * 10^{-14}$ rad^2/s. The slow rotational diffusion of methyl hexanoate was five times slower than that of water and varied less with the distance from the protein.

Structural changes and fluctuations in the protein

The root-mean-square (RMS) distance between the Cα atoms in the simulations and the crystal structure are given in Fig. 6. The RMS distances for all atoms were about 0.5 Å higher. The RMS distances between the simulated average structures and the crystal structure are shown in Table 1. The distances between the simulated structures and the crystal structure increased rapidly in the first 5–10 ps followed by a slow stabilization. After 200 ps the RMS distances to the crystal structure in the VACU, MHEXU and WTRC simulations were close to 2 Å for all atoms and 1.7 Å for the Cα atoms. Notable is the observation that the structures of the VACU and WTRC simulation had similar RMS deviations from the crystal structure after 200 ps of simulation time. However, the VACU simulation had a shorter stabilization time. This resulted in a structure more different from the crystal structure than that of the WTRC simulation in the beginning of the calculations. The structures of the VACC and MHEXC simulations showed the largest RMS deviations. An explanation for this is the absence of electrostatic screening in the vacuum case and the insufficient screening by methyl hexanoate. In a nonpolar solvent such as methyl hexanoate some of the potentially charged residues on the surface of the protein probably have such protonation states that they do not carry net charges.

The distance between each Cα atom of the averaged WTRC structure and the crystal structure is shown in Fig. 7. There were several regions in the sequence that had high deviations up to 3 Å. These deviations frequently occurred in hairpin loops at the surface of the protein. If these loops were excluded from the calculations, the RMS distance of the remaining Cα atoms to those of the crystal structure was as low as 1.1 Å in the WTRC simulation.

TABLE 1 RMS distances (Å) of all atoms between the average simulated structures and the crystal structure of the lipase

	VACU	VACC	MHEXU	MHEXC	3TGL
WTRC	2.6	3.6	2.4	3.0	1.9
VACU		2.6	2.4	3.5	2.4
VACC			3.7	3.8	3.6
MHEXU				3.2	2.0
MHEXC					3.0

Names are based on the entry number in the Brookhaven Protein Data Bank. Molecular dynamics structures are averaged over 150 ps.

The RMS deviations between the crystal structure and the simulated structures originated partly from shortcomings in the simulation techniques such as inaccuracies in the force fields. Some of the deviations were certainly due to the differences in the environments of the simulated protein and the crystal structure. In the Brookhaven Protein Data Bank (Bernstein et al., 1977; Abola et al., 1987) there are two fairly large proteins, lysozyme and interleukin-1β, for which the structures have been determined both by x-ray crystallography (Diamond, 1974; Priestle et al., 1989; Veerapandian et al., 1992) and in solution by NMR spectroscopy (Clore et al., 1991; Smith et al., 1993). The RMS distances for all atoms between the structures in solution and the crystal structures are 2.4 and 1.7 Å for the two proteins, respectively. The RMS distance between the averaged WTRC structure and the crystal structure of the lipase was 1.9 Å. With current knowledge it is not easy to say to what extent the deviations in the simulations are caused by imperfections in the calculations and/or by differences in the environment.

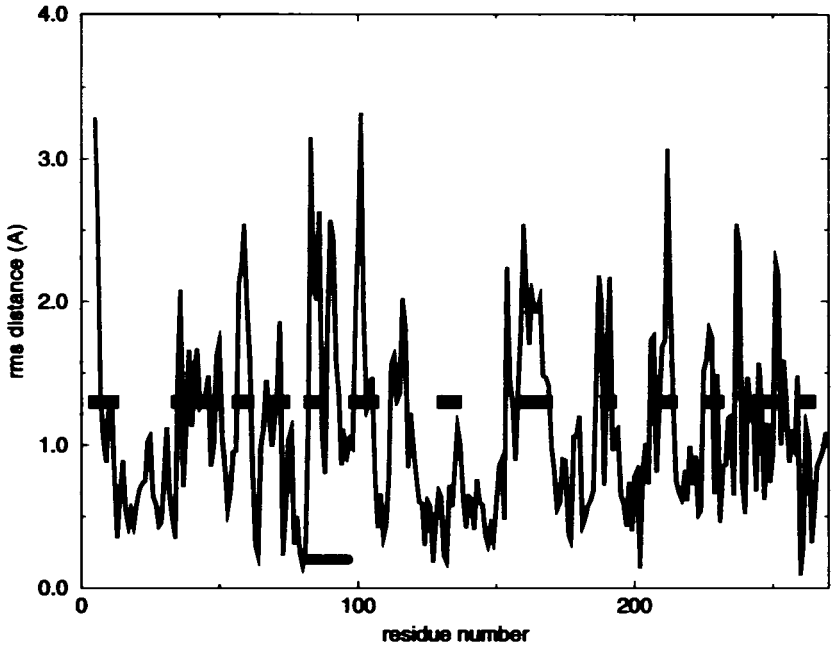

FIGURE 7 Distances between the Cα atoms of the average simulated WTRC structure and the crystal structure. Hairpin loops on the surface of the protein are marked with bars. The lid region is marked with a bar with rounded corners.

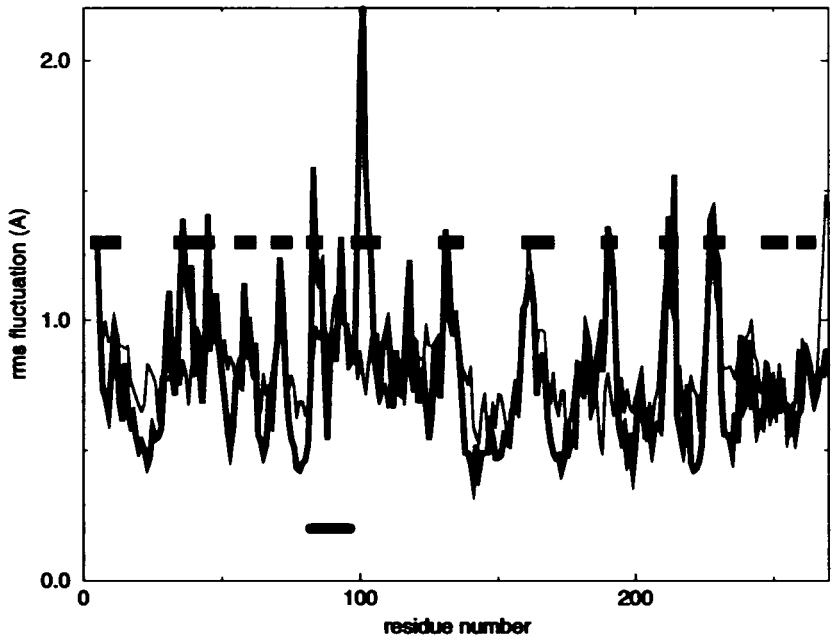

FIGURE 8 The fluctuations of Cα atoms in the WTRC simulation are shown with a thick line. The fluctuations of the crystal structure are calculated from temperature factors and shown with a thin line. Hairpin loops on the surface of the protein are marked by bars. The lid region is marked with a bar with rounded corners.

The fluctuations of the Cα atoms in the WTRC and MHEXC simulations are shown against residue number in Fig. 8. Residues with large fluctuations coincide with hairpin loops at the surface and with regions where large RMS deviations to the crystal structure were observed. The values obtained by simulation agreed well with the fluctuations calculated from the crystallographic temperature factors except for a large peak in the fluctuations in the simulations at Pro100 and Pro101, which is absent in the experimental temperature factors (Fig. 8). Pro100 is involved in direct crystal contacts, including hydrogen bonding to another protein molecule in the crystal structure (Derewenda et al., 1992a). This will obviously give rise to smaller fluctuations in the crystal structure. In addition, these residues belong to the hinge region of the protein, which undergoes a large conformational change upon activation of the enzyme (Brzozowski et al., 1991). There were two other smaller peaks in the fluctuations that have no counterparts in the experimental temperature factors. These were at residues 36 and 190–191. Both were in external loops and in both cases there were also peaks in the RMS distance to the crystal structure with heights just above 2 Å.

The average RMS fluctuations are given in Table 2. The flexibility of the protein was highest in the water simulation and lowest in the VACC simulation followed by the MHEXC simulation. Levitt and Sharon (1988) observed an increase in

TABLE 2 RMS fluctuations (Å)*

Simulation	All Atoms	Cα
VACC	0.84	0.65
VACU	1.01	0.67
MHEXC	0.93	0.74
MHEXU	1.02	0.76
WTRC	1.14	0.84
Experimental‡	0.90	0.83

* Averaged over 150 ps.
‡ Experimental fluctuations are calculated from crystallographic temperature factors of the lipase.

the fluctuations of protein atoms in a vacuum simulation compared with one in water, which is contradictory to our results. Spectroscopic studies of protein dynamics (Careri et al., 1980; Goldanskii and Krupyanskii, 1989; Steinhoff et al., 1989) have shown that the intramolecular mobility of a protein interacting with water is higher than in a dry protein. It has been proposed that proteins become more rigid in organic solvents (Waks, 1986; Dordick, 1989; Gupta, 1992). Recently, Fitzpatrick et al. (1993) determined the crystal structure of subtilisin in an organic solvent and observed a reduction of the average temperature factor by 25% compared with the crystal structure in water. The reduction of the fluctuations in the MHEXC simulation compared with the WTRC simulation was about 18%. Although our simulations did not exactly mirror the conditions in the x-ray crystallographic experiments, the lowered RMS fluctuations observed in the nonaqueous simulations confirm the hypothesis that proteins are more rigid in a hydrophobic environment than in water. The origins of this effect will be discussed below.

The radius of gyrations of the simulated structures are given against simulation time in Fig. 9. The proteins shrank compared with the crystal structure in the vacuum simulations. The inclusion of solvent caused a slight swelling, which was largest in the WTRC simulation and smallest in the MHEXU simulation.

Characterization of the changes in the protein structures

The changes of the overall structure of the lipase were studied by calculations of surface areas using the program ACCESS (Lee and Richards, 1971). As seen in Table 3 the total exposed surface areas decreased by 10–13% in the vacuum simulations, whereas they increased in the simulations with solvent. The increase of surface area was 14% in the WTRC simulation, while simulations in methyl hexanoate only caused a 2–4% increase in surface area. The amino acid residues were divided into three classes. These classes were charged (asp, glu, arg, and lys), hydrophilic (ser, thr, his, asn, and gln), and hydrophobic (gly, ala, val, leu, iso, met, cys, phe, tyr, and trp) residues. In the vacuum simulations, the reduction in surface areas were differently distributed depending on the protonation state of the protein. In the VACC simulation the reduction in surface area was largest for the charged residues. The shielding of the charged residues was so strong that the surface area of the hydrophobic residues increased. In the VACU simulation the decrease in surface area was more uniformly distributed, and the reduction in surface area was largest for the hydrophobic residues. In water and methyl hexanoate the protein behaved differently. The charged and polar residues increased their surface area in water, whereas it was the hydrophobic residues that increased their surface area in the MHEXC simulation. The changes in surface area were not only of opposite sign but also smaller in methyl hexanoate than in water.

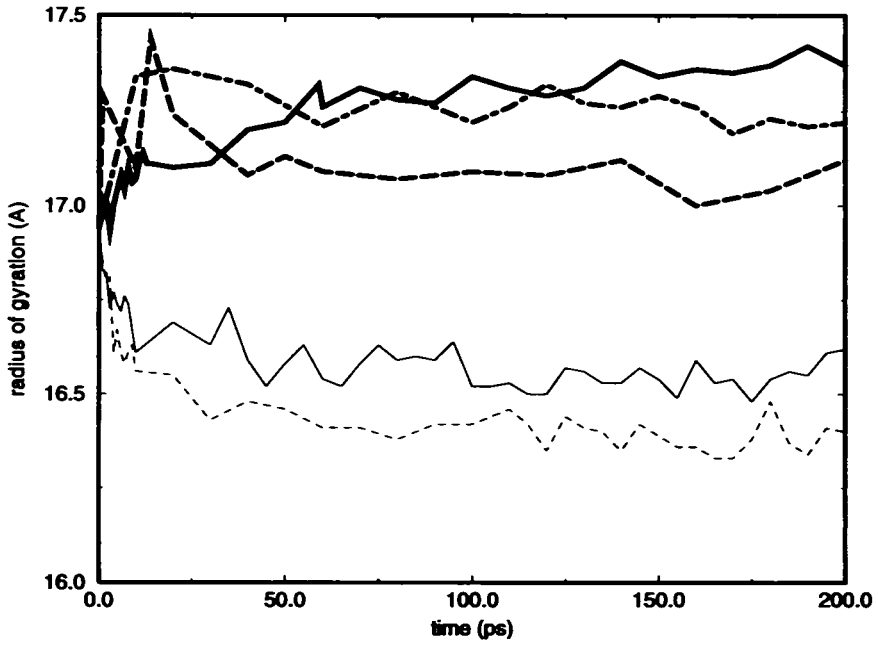

FIGURE 9 Radius of gyration as a function of time in the simulations. Solid thick line is WTRC, solid thin line is VACU, dashed thin line is VACC, dashed thick line is MHEXU, and dashed/dotted line is MHEXC.

TABLE 3 Changes (%) in exposed surfaces compared with corresponding crystal structures and changes (%) in number of hydrogen bonds

	Structures						
	VACC	VACU	MHEXC	MHEXU	WTRC	NMR1‡	NMR2§
Surfaces							
All atoms	−10	−13	+2	+4	+14	+14	+10
Charged residues‖	−33	−12	−8	+14	+36	+21	+16
Hydrophilic residues¶	−16	−7	−1	−1	+12	+2	+5
Hydrophobic residues**	+8	−17	+9	+1	+1	+15	+10
Hydrogen bonds	+57	+23	+27	+14	−10	−12	−16

* Surfaces for the simulated structures are calculated as average structures of 150 ps. Number of hydrogen bonds are calculated from final structures.
‡ Reference structure is averaged over the crystal structures 1lyz, 2lyz, 3lyz, 4lyz, 5lyz, 6lyz, 7lyz, and 8lyz in the Protein Data Bank. The code for the NMR structure is 1hwa.
§ Crystal structure is 2i1b. NMR structure is 6i1b.
‖ Asp, Glu, Arg, and Lys.
¶ Ser, Thr, Asn, Gln, and His.
** Ala, Val, Trp, Phe, Tyr, Ile, Leu, Met, Pro, Cys, and Gly.

In principle the change of protein surfaces in going from a crystal structure to an aqueous solution structure could be studied by comparing crystal structures with the corresponding NMR structures. Unfortunately, such an investigation is at present limited by the small number of available full-sized proteins of which structures are determined by both means. Nevertheless, we included such an analysis of two proteins, lysozyme (129 a.a residues) and interleukin-1β (153 a.a residues) in Table 3. The difference in surface area between crystal and the solution structures of these two proteins were similar to the difference between the WTRC structure and the crystal structure of the lipase. The increase in surface area of charged residues is about half that in our simulation. The main difference is, however, that in our WTRC simulation the hydrophobic residues had an almost unchanged surface area, whereas the hydrophobic residues of the NMR structures surprisingly increased their surface areas even more than the uncharged hydrophilic residues.

A comparison of the number of intramolecular hydrogen bonds in the structures is shown in Table 3. There are significant differences between the simulations. In water the protein lost 10% of the internal hydrogen bonds compared with the starting crystal structure. The corresponding values for the two comparisons of crystal and NMR structures, lysozyme and interleukin-β, were −12 and −16%, respectively. In the MHEXC, MHEXU, VACC and VACU simulations the number of internal hydrogen bonds increased. If these results are compared with the surface calculations above, some of the molecular mechanisms of the hydrophobic and hydrophilic effects may be explained. The hydrophobic conditions in the methyl hexanoate and vacuum simulations favored close contacts between polar atoms of the protein leading to a diminished exposure of charged and hydrophilic residues. The water solvent was able to replace polar intramolecular interactions favoring exposure polar residues.

Berendsen et al. (1992) recently simulated phospholipase A_2 at the surface of a phospholipid monolayer. They introduced a polarity index, I_{el}, as follows: $I_{el} = (E_{el} - E_{LJ})/(E_{el} + E_{LJ})$. E_{el} is the total electrostatic energy of the system and E_{LJ} is the Lennard-Jones energy. Positive values of I_{el} reflect hydrophilic interactions, i. e., that electrostatic interactions dominate the cohesive energy of the system. Negative values occur in a situation where the system is mainly kept together by Lennard-Jones forces. The values of the polarity index in our simulations are given in Table 4. The strongest polar interactions were those between water molecules. The index value exceeded 1.0, which reflected that the polar contacts forced the Lennard-Jones energy to be repulsive. As expected the most hydrophobic interactions were observed between methyl hexanoate molecules, followed by protein/methyl hexanoate interactions. A comparison between VACC, WTRC, and MHEXC in which the same force field was used showed that the interactions between the atoms of the protein became more polar when the protein was surrounded by the hydrophobic solvent or by vacuum. The polarity indexes obtained for the protein/protein interactions from the vacuum simulations were close to those of the corresponding simulations in methyl hexanoate. Our results are qualitatively in agreement with the corresponding values of Berendsen et al. (1992). In their simulation the protein/protein and the protein/water interactions were more polar than in our simulations, which might reflect differences in the overall hydrophobicity of the simulated proteins. They found a polarity index for lipid-lipid interactions which was about 0.5. This value was higher

TABLE 4 Calculated values of the polarity indexes*

	Type of Interaction		
	Protein/Protein	Protein/Solvent	Solvent/Solvent
Simulation			
VACC	0.42		
VACU	0.00		
MHEXC	0.38	−0.59	−0.96
MHEXU	0.03	−0.72	−0.96
WTRC	0.16	0.69	1.36

* See text for explanation of polarity index. Values are calculated as averages of the last 150 ps of the simulation.

than our value for the methyl hexanoate interactions. This difference may originate from strong polar interactions between the polar heads of the phospholipid, which were weaker for methyl hexanoate.

Structure of the active site region

Because of the predicted conformational change during activation of the lipase it was interesting to examine structural changes in active site region. Lipases are activated by the hydrophobic interface formed by their water insoluble ester substrates (Sarda and Desnuelle, 1958). By crystallographic studies (Brady et al., 1990; Brzozowski et al., 1991; Winkler et al., 1990; van Tilbeurgh et al., 1992; Schrag et al., 1991; and Grochulski et al., 1993) the activation of lipases has been explained by conformational changes. All of the structurally determined true lipases have their active sites buried under one or a few surface loops, which must be displaced to expose the active site of the enzyme to the substrate. Upon activation these loops roll away from the active site resulting in an exposed active site together with a large increase in the hydrophobic surface area of the enzyme (Brzozowski et al., 1991; van Tilbeurgh et al., 1992, Grochulski et al., 1993). In the *R. miehei* lipase the covering surface loop consists of an amphiphilic helix, which moves about 7 Å going from the closed to the open conformation. The lipase is believed to be stabilized in its closed conformation in water, while a hydrophobic environment favors the opening of the active site.

The structure of the lipase after 200 ps in the WTRC and the MHEXC simulations are shown in Fig. 10. In the WTRC simulation the lid remained closed throughout the simulation. Interestingly, in both the MHEXC and the MHEXU simulations one part of the lid began to open forming a hydrophobic groove. One of the methyl hexanoate molecules moved into this groove and approached the active site. However, the lid did not open completely, which prevented the methyl hexanoate molecule to reach the active site residues involved in catalysis.

DISCUSSION

This work may be divided into two sections: the protein effects on the surrounding solvent, and the solvent effects on the protein. The effect of the protein surface on the surrounding solvent was small, and there were only a few more or less bound solvent molecules. The mobility of the nonbonded water molecules in a 5-Å shell around the protein was reduced, but the molecules were able to move more than 5 to 10 Å within 100 ps. For the larger methyl hexanoate molecules such motions were two to three times slower than those of water. The rotational diffusion of the water molecules is reduced more than the translational diffusion. The effect on methyl hexanoate was similar on the two types of motion. Experimental data of water diffusion around hemoglobin (Steinhoff et al., 1993) agreed qualitatively with the water/lipase simulation.

The RMS fluctuations showed that the protein was more rigid in methyl hexanoate than in water. The low intramolecular mobility of proteins in organic solvents has been proposed from experimental results. Porcine pancreatic lipase, in which the active site is composed of flexible loops, was shown to be unable to catalyze interesterifications of large

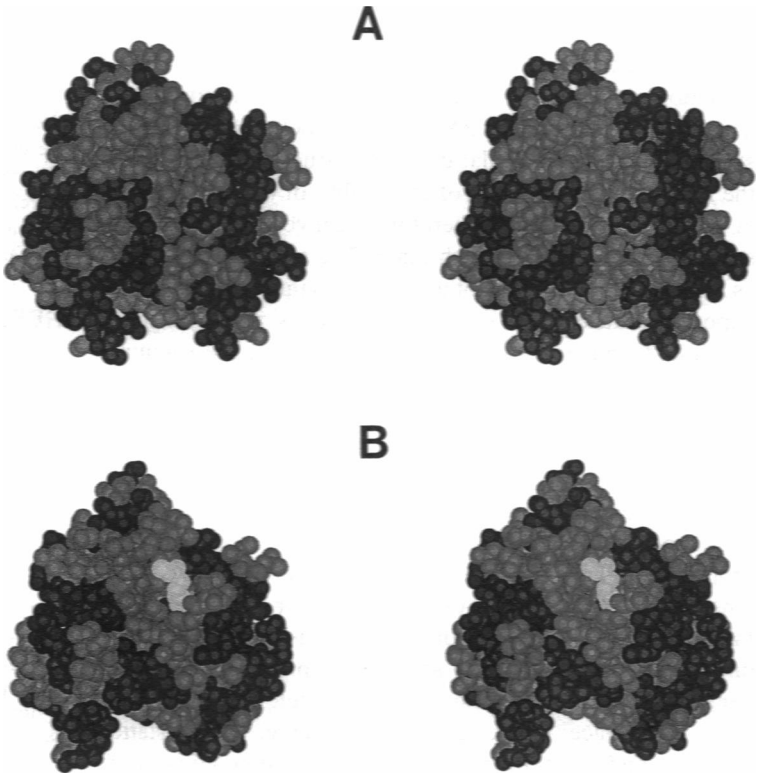

FIGURE 10 Stereopictures of the conformation of the lipase after 200 ps of simulation. Hydrophobic residues are colored dark gray and black. (*A*) The WTRC simulation. (*B*) The MHEXC structure. A methyl hexanoate molecule is shown in light gray. The lid is situated to the right of the methyl hexanoate molecule.

substrates in almost dry tributyrin (Zaks and Klibanov, 1984). Addition of water activated the enzymic reaction. However, smaller substrates reacted both with and without addition of extra water. Rearrangements of the flexible loops at the active site were believed to be important for catalysis of large substrates. However, smaller substrates were accepted by the enzyme without conformational changes. Low intramolecular mobility has also been taken as an explanation for the increased thermostability of enzymes in organic solvents (Zaks and Klibanov, 1984). A comparison of temperature factors of an enzyme crystallized in water and in an organic solvent (Fitzpatrick et al., 1993) showed smaller values of the temperature factors in the organic solvent. The origin of this phenomenon may be found in two effects seen in our simulations. The electrostatic interactions in general become stronger between atoms at the surface of the protein because of weaker shielding in an organic solvent than in water. Further, the number of intramolecular hydrogen bonds, which are of electrostatic character, increases in the organic solvent.

It is apparent, as noted by other authors (Levitt and Sharon, 1988; Van Gunsteren and Mark, 1992) that the inclusion of water improves the agreement of simulated protein structures with crystal structures. The most important contribution of the inclusion of water is the screening of electrostatic interactions. Other ways to model the screening are replacing net charges with dipoles, as in the D version of the GROMOS force field, or to use a distance-dependent dielectric constant (Weiner et al., 1984). In our simulations the first of these approaches was almost as effective in preserving the crystal structure as the inclusion of water. Various approaches to model screening in vacuum have been extensively tested (Nilsson, 1991), and it has been found that removal of net charges gives good results.

Experimental structures of proteins in water solution show deviations in the order of 2 Å from the crystal structures. Thus, a comparison of the RMS distances between the crystal structure and the molecular dynamics structures may not be the most relevant measure of the quality of the simulations at this level of resolution. Therefore, we investigated how the structures differed from each other. The size of the protein as measured by the radius of gyration was important, as were exposed surface areas of various residues and hydrogen bonding. Compared with the crystal structure, the vacuum structures shrank significantly, whereas the solution structures tended to swell slightly (more in water and less in methyl hexanoate). This was not only seen from the radius of gyration but also from changes in the total exposed surfaces. However, the origin of the expansion was different in water and methyl hexanoate. It was the charged and the hydrophilic residues that increased their surface areas in water, whereas the surface area of the hydrophobic residues remained constant. In the organic solvent, the result depended on the assumed protonation state of the protein but was in general opposite to the simulation in water. For quantities such as surface areas, hydrogen bonding, electrostatic screening and size of the protein, the vacuum simulations and the water simulations were extremes. The simulations including the nonpolar solvent formed intermediate cases. The methyl hexanoate simulations were closer to the water simulations for the size of the protein, but closer to the vacuum simulations for the electrostatic screening and intermediate when hydrogen bonding was considered.

In the simulations the lid covering the active site remained closed in water. In methyl hexanoate the lid partly opened exposing a hydrophobic groove in the substrate binding region. Although the lid did not open completely in the hydrophobic solution this result agrees with earlier findings (Derewenda et al., 1992b; Norin et al., 1993) that the lid is stabilized by a hydrophobic environment.

The molecular dynamics simulations in methyl hexanoate showed that the method can be useful in investigating enzyme structure and function in organic solvents. The simulations might be improved by taking into account strongly bonded water molecules, which are not replaced by the organic solvent. These water molecules might be traced by crystallographic studies in organic solvents (Fitzpatrick et al., 1993) or by a molecular dynamics study in water. Strongly bonded water molecules can be important for stabilizing the structure of the enzyme in an organic solvent. However, the time scales normally achievable for molecular dynamics simulations are too short for probing protein unfolding and stability. Another improvement is to treat the protonation states of the charged amino acids rigorously. Charged groups that are not stabilized by ion bridges or dipoles probably have perturbed pKa values in a hydrophobic environment compared with an environment of water molecules. These groups can be traced by electrostatic calculations using the Poisson-Boltzmann equation, which has been used to calculate pKa values of amino acid residues of bacteriorhodopsin inserted in a hydrophobic membrane (Bashford and Gerwert, 1992).

We thank the crystallographic group at the University of York for providing the crystal structures of the lipase. Financial support from the Swedish Research Council for Engineering Science, Swedish Natural Science Research Council and the Swedish Board for Technical Development are gratefully acknowledged. Torbjörn Norin at the Department of Organic Chemistry at KTH is acknowledged for valuable comments.

REFERENCES

Abola, E., F. C. Bernstein, S. H. Bryant, T. F. Koetzle, and J. Weng. 1987. Data Commission of the International Union of Crystallography. Bonn/Cambridge/Chester. 107–132.

Bashford, D., and K. Gerwert. 1992. Electrostatic calculations of the pK_a values of ionizable groups in bacteriorhodopsin. *J. Mol. Biol.* 224: 473–486.

Berendsen, H. J. C., B. Egberts, S.-J. Marbrink, and P. Ahlström 1992. Molecular dynamics simulations of phospholipid membranes and their interaction with phospholipase A_2. *In* Membrane Proteins: Structures, Interactions and Models. A. Pullman et al., editors. Kluwer Academic Publishers, Leiden University, The Netherlands. 457:470.

Berendsen, H. J. C., J. P. M. Postma, W. F. van Gunsteren, and J. Hermans 1981. Interaction models for water in relation to protein hydration. *In* Intermolecular Forces. B. Pullman, editor. Riedel, Dordrecht, Holland.

Bernstein, F. C., T. F. Koetzle, G. J. B. Williams, E. F. Meyer, M. D. J. Brice, J. R. Rodgers, O. Kennard, T. Shimanouchi, and M. Tasumi. 1977. The

Protein Data Bank: A computer-based archival file for macromolecular structures. *J. Mol. Biol.* 112:535–542.

Brady, L., A. M. Brzozowski, Z. S. Derewenda, E. Dodson, G. Dodson, S. Tolley, J. P. Turkenburg, L. Christiansen, B. Huge-Jensen, L. Norskov, L. Thim, and U. Menge. 1990. A serine protease triad forms the catalytic centre of a triacylglycerol lipase. *Nature* 343:767–770.

Brooks, B. R., R. E. Bruccoleri, B. D. Olafson, D. J. States, S. Swaminathan, and M. Karplus. 1983. CHARMM: A program for macromolecular energy, minimization, and dynamics calculations. *J. Comput. Chem.* 4:187–217.

Brooks III, C. L., and M. Karplus. 1989. Solvent effects on protein motion and protein effects on solvent motion. Dynamics of the active site region of lysozyme. *J. Mol. Biol.* 208:159–181.

Brzozowski, A. M., U. Derewenda, Z. S. Derewenda, G. G. Dodson, D. M. Lawson, J. P. Turkenburg, F. Bjorkling, B. Huge-Jensen, S. A. Patkar, and L. Thim. 1991. A model for interfacial activation in lipases from the structure of a fungal lipase-inhibitor complex. *Nature* 351:491–494.

Careri, G., E. Gratton, P.-H. Yang, and J. A. Rupley. 1980. Correlation of IR spectroscopic, heat capacity, diamagnetic susceptibility and enzymatic measurements on lysozyme powder. *Nature* 284:572–573.

Clore, G. M., P. T. Wingfield, and A. M. Gronenborn. 1991. High resolution three-dimensional structure of interleukin 1β in solution by three- and four-dimensional nuclear magnetic resonance spectroscopy. *Biochemistry* 30:2315–2323.

De Loof, H., L. Nilsson, and R. Rigler. 1992. Molecular dynamics simulations of galanin in aqueous and nonaqueous solution. *J. Am. Chem. Soc.* 114:4028–4035.

Derewenda, Z. S., U. Derewenda, and G. G. Dodson. 1992a. The crystal and molecular structure of the *Rhizomucor miehei* triacylglyceride lipase at 1.9 Å resolution. *J. Mol. Biol.* 227: 818–839.

Derewenda, U., A. M. Brzozowski, D. M. Lawson, and Z. S. Derewenda. 1992b. Catalysis at the interface: the anatomy of a conformational change in a triglyceride lipase. *Biochemistry* 31:1352–1541.

Diamond, R. 1974. Real-space refinement of the structure of hen egg-white lysozyme. *J. Mol. Biol.* 82:371–391.

Dordick, J. S. 1989. Enzymatic catalysis in monophasic organic solvents. *Enzyme Microb. Technol.* 11:194–211.

Fitzpatrick, P. A., A. C. U. Steinmetz, D. Ringe, and A. M. Klibanov. 1993. Enzyme crystal structure in a neat organic solvent. *Proc. Natl. Acad. Sci. USA.* 90:8653–8657.

Goldanskii, V. I., and Y. F. Krupyanskii. 1989. Protein and protein-bound water dynamics by Rayleigh scattering of Mössbauer radiation (rsmr). *Q. Rev. Biophys.* 22:39–92.

Grochulski, P., Y. Li, J. D. Schrag, F. Bouthillier, P. Smith, D. Harrison, B. Rubin, and M. Cygler. 1993. Insights into interfacial activation from an open structure of *Candida rugosa* lipase. *J. Biol. Chem.* 268: 12843–12847.

Gupta, M. N. 1992. Enzyme function in organic solvents. *Eur. J. Biochem.* 203:17–24.

Hermans, J., H. J. C. Berendsen, W. F. van Gunsteren, and J. P. M. Postma. 1984. A consistent empirical force field for water-protein interactions. *Biopolymers* 23:1513–1518.

Hrovat, M., I. Mirko, and C. G. Wade. 1980. Absolute measurements of diffusion coefficients by pulsed nuclear magnetic resonance. *J. Chem. Phys.* 73:2509–2510.

Janssen, A. J. M., A. J. H. Klunder, and B. Zwanenburgh. 1991. Resolution of secondary alcohols by enzyme-catalyzed transesterification in alkyl carboxylates as the solvent. *Tetrahedron* 47:7645–7662.

Jorgensen, W. L., and J. Tirado-Rives. 1988. The OPLS potential function for proteins. Energy minimizations for crystals of cyclic peptides and crambin. *J. Am. Chem. Soc.* 110:1657–1666.

Klibanov, A. M. 1986. Enzymes that work in organic solvents. *CHEMTECH.* 63:354–359.

Komeiji, Y., M. Uebayasi, J. Someya, and I. Yamato. 1993. A molecular dynamics study of solvent behavior around a protein. *Proteins Struct. Funct. Genet.* 16:268–277.

Lautz, J., H. Kessler, W. F. van Gunsteren, H.-P. Weber, and R. M. Wenger. 1990. On the dependence of molecular conformation on the type of solvent environment: a molecular dynamics study of cyclosporin A. *Biopolymers.* 29:1669–1687.

Lee, B., and F. M. Richards. 1971. Interpretation of protein structures: Estimation of static accessibility. *J. Mol. Biol.* 55:379–400.

Levitt, M., and R. Sharon. 1988. Accurate simulation of protein dynamics in solution. *Proc. Natl. Acad. Sci. USA.* 85:7557–7561.

Månsson, M., P. Sellers, G. Stridh, and S. Sunner. 1977. Enthalpies of vaporization of some 1-substituted *n*-alkanes. *J. Chem. Thermodynamics* 9:91–97.

Nilsson, O. 1991. Molecular dynamics modelling of bacteriophage T4 glutaredoxin. Accessing structural stability: computer simulation experiments and their comparison with x-ray diffraction data. Ph.D. thesis. University of Stockholm, Swedea. 214 pp.

Norin, M., O. Olsen, A. Svendsen, O. Edholm, and K. Hult. 1993. Theoretical studies of *Rhizomucor miehei* lipase activation. *Protein Eng.* 6:855–863.

Ollis, D. L., E. Cheah, M. Cygler, B. Dijkstra, F. Frolow, S. M. Franken, M. Harel, S. J. Remington, I. Silman, J. Schrag, J. L. Sussman, K. H. G. Verschueren, and A. Goldman. 1992. The α/β hydrolase fold. *Protein Eng.* 5:197–211.

Priestle, J. P., H.-P. Schaer, and M. G. Gruetter. 1989. Crystallographic refinement of interleukin 1β at 2:0 angstroms resolution. *Proc. Nat. Acad. Sci. USA.* 86: 9667–9671.

Ryckaert, J.-P., G. Ciccotti, and H. J. C. Berendsen. 1977. Numerical integration of the cartesian equations of motion of a system with constraints: molecular dynamics of n-alkanes. *J. Comp. Phys.* 23:327–341.

Sarda, L., and P. Desnuelle. 1958. Action de la lipase pancréatique sur les esters en émulsion. *Biochim. Biophys. Acta.* 30:513–521.

Schrag, J. D., Y. Li, S. Wu, and M. Cygler. 1991. Ser-His-Glu triad forms the catalytic site of the lipase from *Geotrichum candidum*. *Nature* 351:761–764.

Smith, L. J., M. J. Sutcliffe, C. Redfield, and C. M. Dobson. 1993. Structure of hen lysozyme in solution. *J. Mol. Biol.* 229:930–944.

Sonnet, P. E., and G. G. Moore. 1988. Esterification of 1- and *rac*-2-octanols with selected acids and acid derivatives using lipases. *Lipids* 23:955–960.

Steinhoff, H.-J., B. Kramm, G. Hess, C. Owerdieck, and A. Redhardt. 1993. Rotational and translational water diffusion in the hemoglobin hydration shell: dielectric and proton nuclear relaxation measurements. *Biophys. J.* 65:1486–1495.

Steinhoff, H.-J., K. Lieutenant, and J. Schlitter. 1989. Residual motion of hemoglobin-bound spin labels as a probe for protein dynamics. *Z. Naturforch. Sect. C Biosci.* 44:280–288.

Tripos 1993. Tripos Associates, St. Louis, Missouri. Molecular modelling program SYBYL 6:0.

van Gunsteren, W. F., and H. J. C. Berendsen 1987. GROMOS software manual, Gromos Molecular Simulation, Biomos b.v., Groningen, The Netherlands.

van Gunsteren, W. F., and M. Karplus. 1982. Protein dynamics in solution and in a crystalline environment: a molecular dynamics study. *Biochemistry* 21:2259–2274.

van Gunsteren, W. F., and A. E. Mark. 1992. On the interpretation of biochemical data by molecular dynamics computer simulation. *Eur. J. Biochem.* 204:947–961.

van Tilbeurgh, H., L. Sarda, R. Verger, and C. Cambillau. 1992. Structure of the pancreatic lipase-procolipase complex. *Nature* 359:159–162.

Veerapandian, B., G. L. Gilliland, R. Raag, A. L. Svensson, Y. Masui, Y. Hirai, and T. L. Poulus. 1992. Functional implications of interleukin-1β, based on the three dimensional structures. *Proteins Struct. Funct. Genet.* 12:10–23

Waks, M. 1986. Proteins and peptides in water-restricted environments. *Proteins Struct. Funct. Genet.* 1:4–15.

Wallquist, A., and O. Teleman. 1991. Properties of flexible water models. *Mol. Phys.* 74:515–533.

Weiner, S. J., P. A. Kollman, D. A. Case, U. C. Singh, C. Ghio, G. Alagona, S. Profeta Jr., and P. Weiner. 1984. A new force field for molecular mechanical simulation of nucleic acids and proteins. *J. Am. Chem. Soc.* 106:765–784.

Winkler, F. K., A. D'Arcy, and W. Hunziker. 1990. Structure of human pancreatic lipase. *Nature* 343:771–774.

Wong, C. F., and J. A. McCammon. 1986. Computer simulation and design of new biological molecules. *Isr. J. Chem.* 27:211–215.

Zaks, A., and A. M. Klibanov. 1984. Enzymatic catalysis in organic media at 100°C. *Science* 224:1249–1251.

Zaks, A., and A. M. Klibanov. 1986. Substrate specificity of enzymes in organic solvents vs. water is reversed. *J. Am. Chem. Soc.* 108:2767–2768.